6th European Conference on Computational Mechanics (ECCM 6)
7th European Conference on Computational Fluid Dynamics (ECFD 7)
1115 June 2018, Glasgow, UK

INVESTIGATION OF ADAPTIVE TIME-STEP STRATEGIES FOR HIGH-ORDER ACCURATE INCOMPRESSIBLE SIMULATIONS

G. Noventa[1], F.C. Massa[2], S. Rebay[1], A. Colombo[2], F. Bassi[2] and A. Ghidoni[1]

[1] Università degli Studi di Brescia, Via Branze 38, 25123 Brescia, Italy
{gianmaria.noventa,stefano.rebay,antonio.ghidoni}@unibs.it

[2] Università degli Studi di Bergamo, Viale Marconi 5, 24044 Dalmine (BG), Italy
{francescocarlo.massa,alessandro.colombo,francesco.bassi}@unibg.it

Key words: adaptive time-step strategy, Rosenbrock-type Runge-Kutta schemes, Rosenbrock-type peer schemes, ESDIRK schemes, discontinuous Galerkin, incompressible flows, Navier-Stokes equations, RANS equations

Abstract. Adaptive time-step algorithms can improve considerably the effectiveness of unsteady flow computations. Several adaptive time-step strategies are available in the literature but in all cases conservative time-step choices (small time steps) lead to a large number of time integration steps, while aggressive time-step choices (large time steps) lead to a large number of rejected time integration steps, and in both cases the efficiency and/or robustness of the adaptive strategy may be far from optimal. An appropriate adaptive strategy should instead guarantee both robustness (small-number of rejected time integration steps) and efficiency (small-number of time-integration steps for a given accuracy).

In this work several adaptive time-step strategies have been adopted for the numerical solution of the unsteady incompressible Navier-Stokes and Reynolds-Averaged Navier-Stokes equations based on a high-order accurate discontinuous Galerkin space discretization. Three different classes of time integration methods have been considered, the linearly implicit Rosenbrock-type Runge-Kutta schemes [2], linearly implicit Rosenbrock-type two-step peer schemes [3] and ESDIRK schemes [2]. In oder to assess the adaptive time-step methods for both autonomous and non-autonomous (time-dependent boundary conditions) DAE systems of increasing stiffness, we will present the results obtained in the comuptation of unsteady laminar and turbulent flows around a circular cylinder at increasing Reynolds numbers ranging from $\mathrm{Re} = 100$ to $\mathrm{Re} = 3900$.

1 INTRODUCTION

Discontinuous Galerkin (DG) methods have been emerging as one of the most promising approaches to high-fidelity fluid dynamics computations in many technical areas, including

aeronautics, aeroacoustics and turbomachinery [1]. These kind of simulations usually involve the computation of unsteady flows characterized by a wide range of spatial and temporal scales over (very) long time periods and therefore require efficient, robust and accurate time integration methods.

Standard implicit time integration schemes have been extensively investigated for the solution of the compressible Navier-Stokes equations. Very limited information is instead available on adaptive time step strategies, either for the solution of systems of differential algebraic equations (DAE) such as the incompressible Navier-Stokes equations and for the stiff systems resulting from the discretization of the unsteady Reynolds Average Navier-Stokes equations (URANS) [2].

To cover this gap, this work focuses on the performance of several Runge-Kutta schemes of order of accuracy ranging from three to six — namely linearly implicit one-step Rosenbrock methods, Rosenbrock two-step "peer" schemes, and ESDIRK schemes [3] — as time integrators of the high-order DG space discretization of the incompressible Navier-Stokes (INS) and incompressible Reynolds averaged Navier-Stokes (URANS) equations coupled with the k-$\widetilde{\omega}$ turbulence model [7]. The robustness and efficiency of the time integration schemes is augmented by an adaptive time-step strategy based on a local error estimator which exploits the local truncation error of the time integration scheme and of its lower order embedded scheme.

The paper is organized as follows. Section 2 describes the adaptive time-step algorithm with an overview of the most popular error estimators and controllers available in the literature. Section 3 presents the comparison of the different adaptive time integration strategies for autonomous and non-autonomous problems, namely the unsteady laminar and turbulent flow around a circular cylinder at different Reynolds numbers ranging from $\mathrm{Re} = 100$ to $\mathrm{Re} = 3900$. Section 4 summarizes the main findings and gives some indications for future developments of this work.

2 ADAPTIVE TIME-STEP STRATEGY

Automatic step-size control is an important feature for the efficiency and robustness of time integration schemes. Fixed time steps typically results in a large number of small steps, leading to large simulation costs. Adaptively variable time step can instead substantially improve the simulation effectiveness by (i) reducing the number of time steps — and therefore minimizing the computational effort — required to achieve a user-defined accuracy level and by ($($ii$)$) improving the robustness of the computation as a result of lower local truncation error values during the time integration process.

Following the idea put forward by Söderlind and Wang [8], three different "error types" are needed for an adaptive time integration strategy:

- *Global error* at time t^{n+1}, defined as the difference between the exact $u(t^{n+1})$ and the numerical u^{n+1} solution

$$err^{n+1} = \|u(t^{n+1}) - u^{n+1}\|, \tag{1}$$

  where $\|\cdot\|$ denotes some user defined norm;

- *Local Truncation Error* (LTE), *i.e.* the numerical error introduced by the scheme in a single time step
$$LTE^{n+1} = \|u(t^{n+1}) - u_\star^{n+1}\|, \tag{2}$$
where $u_\star^{n+1}$ is the approximate solution obtained by applying one step of the considered scheme starting from the exact solution $u(t^n)$;

- *Local estimator*, defined in terms of the solution $\hat{u}$ of the so called "embedded scheme",
$$r^{n+1} = \|u^{n+1} - \hat{u}^{n+1}\|. \tag{3}$$

Each quantity can be represented by means of the asymptotic model

$$err^{n+1} = \psi_g^{n+1} (\Delta t)^{q_g}, \tag{4}$$
$$LTE^{n+1} = \psi_l^{n+1} (\Delta t^n)^{q_l}, \tag{5}$$
$$r^{n+1} = \psi_r^{n+1} (\Delta t^n)^{q_r}, \tag{6}$$

where ψ_g, ψ_l, ψ_r are the estimator constants, q_g, q_l, q_r are the estimator order of convergence, $\Delta t^n \equiv t^{n+1} - t^n$, and Δt is the arithmetic mean of the step sizes used during the integration in time, i.e.

$$\Delta t = \frac{1}{N} \sum_{k=1}^{N} \Delta t^{k-1}, \tag{7}$$

with N the number of steps performed up to time t^{n+1}.

The adaptive time-step strategy consists in choosing the step-size Δt so as to obtain a constant LTE during the time integration. However the LTE error cannot be computed when the analytic solution is unavailable and is therefore apprtoximated as $LTE^{n+1} \approx r^{n+1}$. Since LTE depends only (approximately) on r, the adaptive integration strategy chooses Δt in order to keep r equal to a constant value during the time integration.

In practice, the standard adaptive time-step algorithm [8, 9] requires at each time step that

$$LTE^{n+1} \approx r^{n+1} < \mu TOL, \tag{8}$$

where TOL is a user-defined adaptive tolerance and $\mu = \{3/2, 2\}$ is a user-defined safety factor. If this condition is verified the solution u^{n+1} is accepted, and the next step-size Δt^{n+1} is computed using Eq. (6) with $r^{n+2} = TOL$, thus obtaining

$$\Delta t^{n+1} = \left(\frac{r^{n+2}}{\psi_r^{n+2}} \right)^{\frac{1}{q_r}} = \left(\frac{TOL}{\psi_r^{n+2}} \right)^{\frac{1}{q_r}}. \tag{9}$$

Otherwise u^{n+1} is rejected, and the step is repeated with a smaller Δt^n given by

$$\Delta t^n = \left(\frac{TOL}{\psi_r^{n+1}} \right)^{\frac{1}{q_r}}, \tag{10}$$

where the constant ψ_r^{n+1} is obtained from the current local estimator r^{n+1} and the rejected time-step $\overline{\Delta t}^n$, i.e. as

$$\psi_r^{n+1} = \frac{r^{n+1}}{\left(\overline{\Delta t}^n\right)^{q_r}}. \tag{11}$$

The only unknown quantity in the above relations is the estimator constant ψ_r^{n+2} appearing in Eq. (9), which must be therefore effectively predicted by interpolation of the ψ values available at previous time steps. In practice, introducing the logarithmic variable $\tilde{\psi} = \ln(\psi)$, the interpolation can be written as

$$\tilde{\psi}_r^{n+2} \approx \sum_{j=1}^{z} \alpha_j \tilde{\psi}_T^{n+2-j} + \sum_{j=1}^{z} \beta_j \tilde{\psi}_r^{n+2-j}, \tag{12}$$

thus obtaining

$$\psi_r^{n+2} = \prod_{j=1}^{z} \left(\psi_T^{n+2-j}\right)^{\alpha_j} \prod_{j=1}^{z} \left(\psi_r^{n+2-j}\right)^{\beta_j}, \tag{13}$$

where z is the number of past values used, α_j, β_j are real coefficients and

$$\psi_T^{n+2-j} = \frac{TOL}{\Delta t^{n+1-j}}, \qquad j = 1, \ldots, z. \tag{14}$$

Notice that, due to the logarithmic variables, the predicted estimator constant is always positive regardless of the α_j and β_j values. By combining Eq. (13) and Eq.(9), and by considering different sets of α_j and β_j coefficients, the following so called proportional-integral (PI) controllers for the computation of Δt^{n+1} are obtained

$$\Delta t^{n+1} = \Delta t^n \left(\frac{TOL}{r^{n+1}}\right)^{\frac{1}{q_r}}, \tag{15}$$

$$\Delta t^{n+1} = \Delta t^n \left(\frac{\Delta t^n}{\Delta t^{n-1}}\right) \left(\frac{TOL r^n}{r^{n+1} r^{n+1}}\right)^{\frac{1}{q_r}}, \tag{16}$$

$$\Delta t^{n+1} = \Delta t^n \left(\frac{TOL}{r^{n+1}}\right)^{\frac{3}{5q_r}} \left(\frac{r^n}{TOL}\right)^{\frac{1}{5q_r}}, \tag{17}$$

$$\Delta t^{n+1} = \Delta t^n \left(\frac{\Delta t^n}{\Delta t^{n-1}}\right)^{-\frac{1}{4}} \left(\frac{TOL}{r^{n+1}}\right)^{\frac{1}{4q_r}} \left(\frac{TOL}{r^n}\right)^{\frac{1}{4q_r}}, \tag{18}$$

$$\Delta t^{n+1} = \Delta t^n \left(\frac{\Delta t^n}{\Delta t^{n-1}}\right)^{-\frac{3}{8}} \left(\frac{\Delta t^{n-1}}{\Delta t^{n-2}}\right)^{-\frac{1}{8}} \left(\frac{TOL}{r^{n+1}}\right)^{\frac{1}{8q_r}} \left(\frac{TOL}{r^n}\right)^{\frac{1}{4q_r}} \left(\frac{TOL}{r^{n-1}}\right)^{\frac{1}{8q_r}}. \tag{19}$$

The above controllers (15)–(19) are named standard [10], standard$^+$ [5], PI.4.2 [11], H211b [9] and H312b [9], respectively. The coefficients α_j and β_j used in the above controllers are reported in Table 1.

Table 1: Real coefficients α_j and β_j of the formulation (13) for each adaptive time-step controller used in this work. Note that the consistency condition $\sum_{j=1}^{z} \alpha_j + \beta_j = 1$ is always verified.

	z	α_1	α_2	α_3	β_1	β_2	β_3
standard	1	0	-	-	1	-	-
standard$^+$	2	0	0	-	2	-1	-
PI.4.2	2	2/5	1/5	-	3/5	$-1/5$	-
H211b	2	2/4	0	-	1/4	1/4	-
H312b	3	4/8	0	0	1/8	2/8	1/8

Following the idea of Söderlind and Wang [8], the robustness and the efficiency of the adaptive algorithm is substantially improved by limiting the maximum possible increase/reduction of the Δt value by means of the smooth limiter function

$$\Delta t_l^{n+1} = \Delta t^n \left[1 + \kappa \arctan\left(\frac{\Delta t^{n+1} - \Delta t^n}{\kappa \Delta t^n} \right) \right], \tag{20}$$

where Δt_l^{n+1} denotes the limited step-size value used during the next time step. The value of the parameter κ appearing in Eq. (20) must be set in the range $[0.7, 2]$. In this work the effects of the smooth limiter function have been analysed with the H221b controller using $\kappa = 1$.

The target of an adaptive time stepping procedure is to control the global error of the computation, while the parameter that drives the previously described adaptive procedure is the tolerance TOL. It is however possible to devise a procedure so that the tolerance TOL becomes in fact equal to the required global error. This requires an appropriate calibration, see e.g. Söderlind and Wang [8], that must be performed for any time integration shemes before the actual computation.

3 NUMERICAL RESULTS

All the computations have been run on a Linux cluster with 12 AMD 6220 CPUs (8 cores per CPU). The computing time t_{CPU} is reported in the tables as a normalized value with respect to the *TauBenchmark* [12] value, $t_{TauBench}$, obtained on a full node of the cluster used for the CFD simulation[1]. The normalized computing time is measured as work units defined as $wu = (t_{CPU} n_{cores})/t_{TauBench}$, where t_{CPU} is the wall clock time and n_{cores} the numbers of cores.

Different estimators can be built by considering different variables as error indicators. We here consider (i) the estimator of the $x-$component of the velocity field, (ii) the RMS of the velocity components estimators, (iii) the arithmetic mean value of all the unknowns and (iv) the RMS of the estimators all of the unknowns.

3.1 LAMINAR FLOW AROUND A CIRCULAR CYLINDER

The laminar flow around a circular cylinder for a Reynolds number Re = 100, based on the cylinder diameter and the freestream quantities, is here considered. The mesh

[1]-n 250000 -s 10 define the reference TauBench workload for the hardware benchmark.

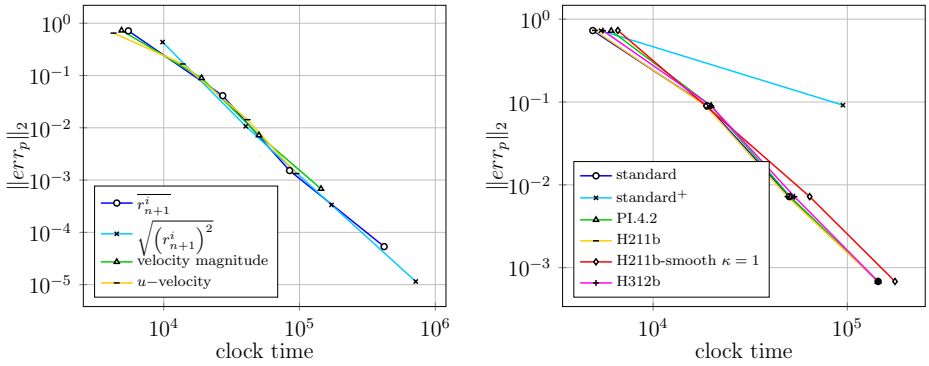

Figure 1: Cylinder $Re = 100$. L^2 norm of the pressure error ($\|err_p\|_2$) as a function of the clock time with different error estimators (left) and controllers (right), ROS3PL scheme with $tol_{system} = 10^{-14}$ and $\mathbb{P}^5$ solution approximation

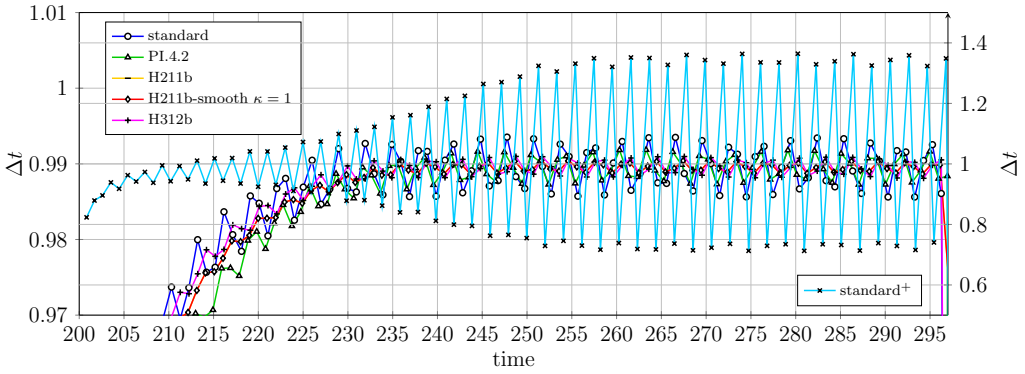

Figure 2: Cylinder $Re = 100$. Time-step Δt evolution with different controllers, ROS3PL scheme with $TOL = 10^{-3}$, $tol_{system} = 10^{-14}$ and $\mathbb{P}^5$ solution approximation

has 5103 hybrid elements, triangles and quadrilaterals, with quadratic edges and it has been generated with a $2D$ high-order version of a fully automated in-house hybrid mesh generator based on the Advancing-Delaunay strategy, a $\mathbb{P}^5$ solution approximation has been used.

All computations have the same initial flow field, created starting from a $\mathbb{P}^1$ steady computation and advancing in time from $\mathbb{P}^1$ to $\mathbb{P}^5$, simulating three shedding for each polynomial degree and using RODASP scheme with the following parameters for the adaptive time-step strategy: $TOL = 10^{-6}$, $tol_{system} = 10^{-14}$. The results are compared with respect to a reference solution (p_{ref}) obtained with ROD5_1 scheme for a simulation time equal to $\Delta t_{sim} = 16T$, where T is the vortex shedding period, and with the following parameters: $\Delta t = T/1632$, $tol_{system} = 10^{-14}$ without the adaptive time-step strategy.

First, the influence of the error estimators and the controllers has been investigated, Fig. 1 shows the performance of different error estimator and controllers with ROS3PL scheme, in terms of the norm of the pressure error as a function of the clock time. While Fig. 2 shows the evolution of the adaptive time-step Δt with $TOL = 10^{-3}$.

With velocity magnitude error estimator and H211b controller the performance of the

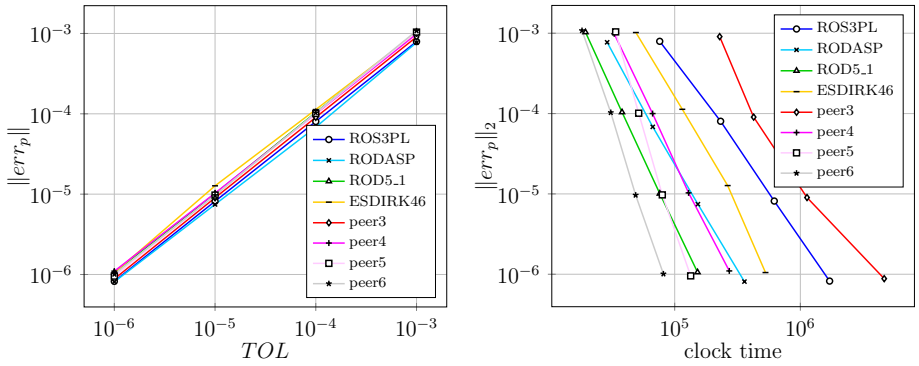

Figure 3: Cylinder $Re = 100$. L^2 norm of the pressure error ($\|err_p\|_2$) as a function of the adaptive tolerance TOL (left) and the clock time (right) after the tolerance calibration procedure, $tol_{system} = \eta TOL$, $tol_{GMRES} = 10^{-2}$ for ESDIRK46 scheme and $\mathbb{P}^5$ solution approximation

schemes has been investigated, Fig. 3 shows the L^2 norm of the pressure error as a function of the adaptive tolerance TOL and the clock time after the calibration procedure. For $\|err_p\|_2 < 10^{-3}$ peer6 scheme is the most efficient, reducing the computational time up to 46% with respect to ROD5_1, at $\|err_p\|_2 \sim 10^{-6}$, while for a higher error ROD5_1 scheme shows similar performance.

3.2 LAMINAR FLOW AROUND A ROTATING CIRCULAR CYLINDER

The influence of time-dependent boundary conditions has been investigated in the case of the laminar circular cylinder. A rotating cylinder has been considered with the same Reynolds number and a speed ratio $\alpha = \omega r / v_\infty = 0.5$, where ω is the rotating velocity, v_∞ the far velocity and r the radius of the cylinder. The governing equations formulated in the non-inertial reference frame [2] have been adopted to take into account the rotation without moving the mesh.

Fig. 4 shows the performance of different error estimators and controllers with ROS3PL scheme, in terms of the norm of the pressure error as a function of the clock time. While Fig. 2 shows the evolution of the adaptive time-step Δt with $TOL = 10^{-3}$, where are different behaviour of the controllers in terms of oscillations. In these laminar testcases each controller and error estimators guarantees the same robustness and performance, except standard$^+$ controller, without any difference between first-, second- and third-order of controllers.

With velocity magnitude error estimator and H211b controller the performance of the schemes has been investigated, Fig. 6 shows the L^2 norm of the pressure error as a function of the adaptive tolerance TOL and the clock-time after the tolerance calibration procedure. peer6 scheme is always better than other schemes, showing comparable performance with ROD5_1 only for high error levels, $\|err_p\|_2 \sim 10^{-2}$, and guarantees a computational saving up to 59% at $\|err_p\|_2 \sim 10^{-5}$.

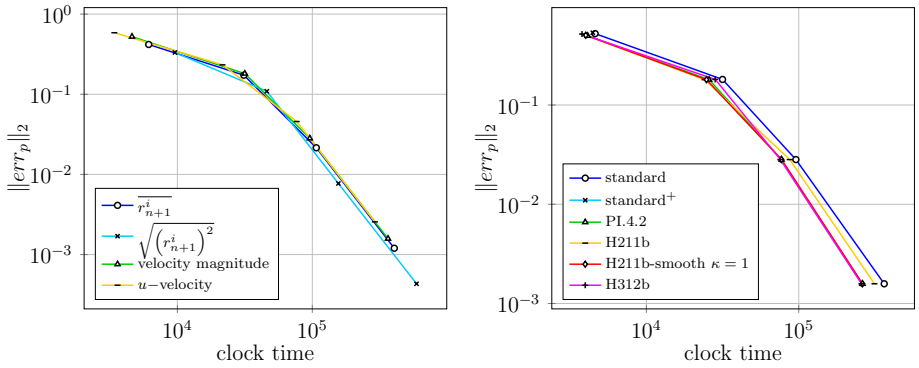

Figure 4: Cylinder $Re = 100$ with $bc(t)$. L^2 norm of the pressure error ($\|err_p\|_2$) as a function of the clock time with different error estimators (left) and controllers (right), ROS3PL scheme with $tol_{system} = 10^{-14}$ and $\mathbb{P}^5$ solution approximation

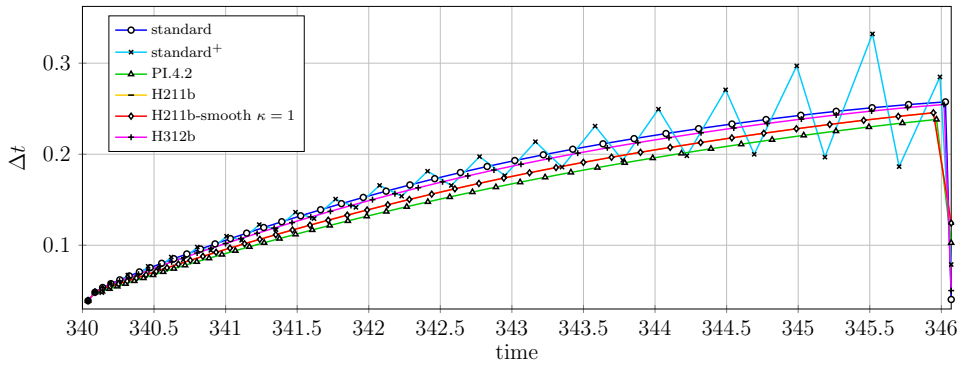

Figure 5: Cylinder $Re = 100$ with $bc(t)$. Time-step Δt evolution with different controller, ROS3PL scheme with $TOL = 10^{-3}$, $tol_{system} = 10^{-14}$ and $\mathbb{P}^5$ solution approximation

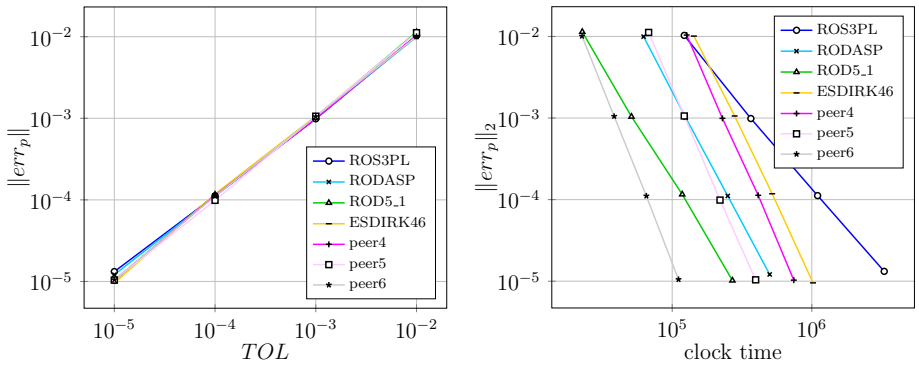

Figure 6: Cylinder $Re = 100$ with $bc(t)$. L^2 norm of the pressure error ($\|err_p\|_2$) as a function of the adaptive tolerances TOL (left) and the clock time (right) after the tolerance calibration procedure, $tol_{system} = \eta TOL$, $tol_{GMRES} = 10^{-2}$ for ESDIRK46 scheme and $\mathbb{P}^5$ solution approximation

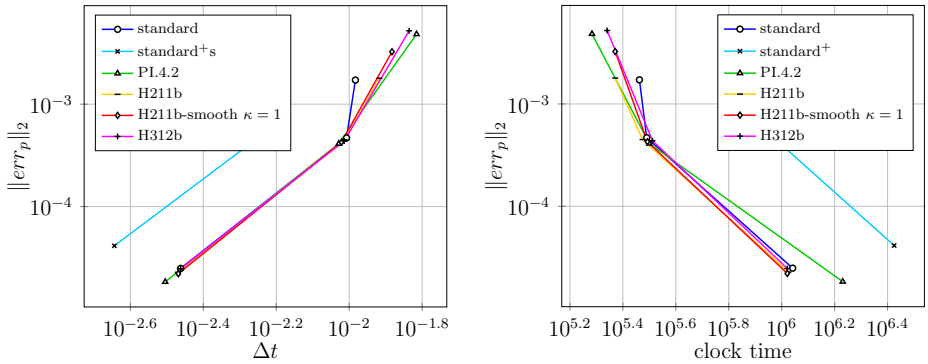

Figure 7: Cylinder $Re = 3900$. L^2 norm of the pressure error ($\|err_p\|_2$) as a function of the time-step Δt (left) and the clock time (right) with different controllers, ROS3PL scheme with $tol_{system} = 10^{-14}$ and $\mathbb{P}^5$ solution approximation

3.3 TURBULENT FLOW AROUND A CIRCULAR CYLINDER

We next consider the turbulent flow around a circular cylinder for a Reynolds number Re = 3900, based on the cylinder diameter and the freestream quantities. The mesh has 4037 hybrid elements, triangles and quadrilaterals, with quadratic edges and it has been generated with a $2D$ high-order version of a fully automated in-house hybrid mesh generator based on the Advancing-Delaunay strategy, a $\mathbb{P}^5$ solution approximation has been considered.

All computations have the same initial flow field, created starting from a $\mathbb{P}^1$ steady computation and advancing in time from $\mathbb{P}^1$ to $\mathbb{P}^5$, simulating one shedding for each polynomial degree and using RODASP scheme with the following parameters for the adaptive time-step strategy: $TOL = 10^{-6}$, $tol_{system} = 10^{-14}$. The results are compared with respect to a reference solution (p_{ref}) obtained with ROD5_1 scheme for a simulation time equal to $\Delta t_{sim} = T$, where T is the vortex shedding period, and with the following parameters: $\Delta t = T/1632$, $tol_{system} = 10^{-14}$ without the adaptive time-step strategy.

For turbulent flows all the variables must be under control by the error estimator, *i.e.* the estimators based on the $x-$component of the velocity and on the velocity magnitude can't be used, while the average error estimator can't guaranteed robustness in the tolerance range $10^{-3} < \|err_p\|_2 < 10^{-6}$. For these reasons the RMS error estimator is the only used, where also the turbulence model variables k and $\tilde{\omega}$ must be taken into account.

Fig. 7 shows the performance of the different controller with ROS3PL scheme, in terms of the norm of the pressure error as a function of the time-step Δt and the clock time. While Fig. 8 shows the evolution of the adaptive time-step Δt and the error estimator r_{n+1} with $TOL = 10^{-5}$.

With H211b controller the performance of the schemes has been investigated, Fig. 9 shows the L^2 norm of the pressure error as a function of the adaptive tolerance TOL and the clock time after the tolerance calibration procedure. For $\|err_p\|_2 < 10^{-5}$ peer5 scheme is the most efficient, reducing the computational time up to 30% with respect to RODASP, which is the best scheme for lower accuracy ($\|err_p\|_2 > 10^{-5}$).

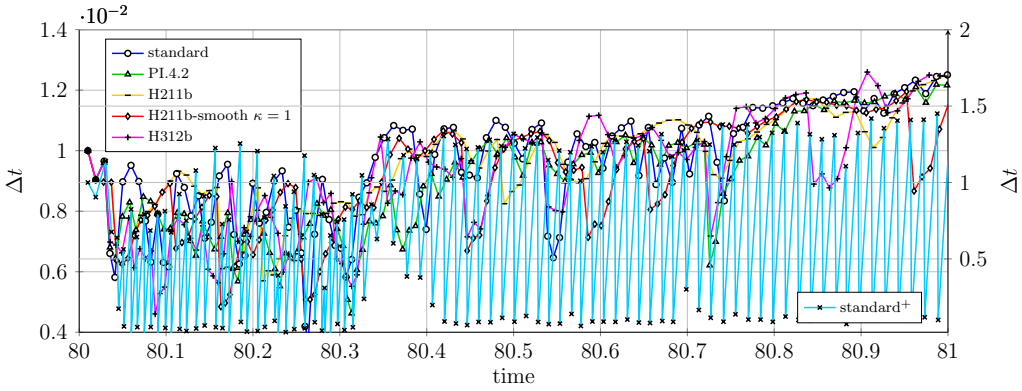

Figure 8: Cylinder $Re = 3900$. Time-step Δt evolution with different controller, ROS3PL scheme with $TOL = 10^{-5}$, $tol_{system} = 10^{-14}$ and $\mathbb{P}^5$ solution approximation

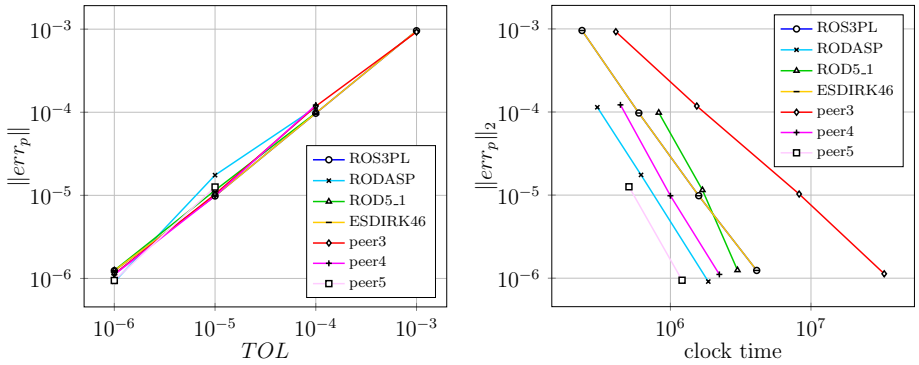

Figure 9: Cylinder $Re = 3900$. L^2 norm of the pressure error as a function of the adaptive tolerances TOL (left) and the clock time (right) after the tolerance calibration procedure, $tol_{system} = \eta TOL$, $tol_{GMRES} = 10^{-2}$ for ESDIRK46 scheme and $\mathbb{P}^5$ solution approximation

4 CONCLUSIONS

In this work a high-order accurate discontinuous Galerkin space discretization coupled with an adaptive time integration algorithm is investigated for the numerical simulation of the incompressible Navier-Stokes and RANS equations with $k - \omega$ turbulence model closure. Three different classes of time integration methods have been considered: the linearly implicit Rosenbrock-type Runge-Kutta schemes, the linearly implicit Rosenbrock-type two-step peer schemes and the ESDIRK schemes.

Traditional controllers and error estimators for adaptive strategies available in the literature have been compared in terms of robustness, accuracy and computational efficiency on several testcases. Autonomous and non-autonomous problems, i.e. problems with time-dependent boundary conditions, have been considered: the unsteady laminar and turbulent flow around a circular cylinder at different Reynolds numbers ranging from Re = 100 to Re = 3900.

For the considered laminar testcases, the different adaptive strategies displayed similar accuracies and computational efficiencies, for the first-, second- and third-order controllers

(with the only exception of the standard$^+$ controller). Notice however that for the turbulent test case the error estimator must be based on all the variables. Peer schemes outperform the one-step traditional methods for almost every level of accuracy. As an example, in the cylinder testcase peer5 shows a computational saving up to $\sim 40\%$ with respect to ROD5_1. Moreover, the peer4 scheme performs similarly to the higher-order accurate RODASP scheme, as peer5 does in comparison to ROD5_1. The lower order schemes, ROS3PL and peer3, show the worst performance due to the lower time-step that introduces an high number of rejected time-step.

Work is in progress to extend the comparison of the performance of the adaptive strategies to other incompressible turbulent test cases, possibly considering problems of industrial relevance, such as the turbulent flow around a circular cylinder at $\mathrm{Re} = 1.4 \times 10^5$ and the turbulent flow through a wind turbine.

REFERENCES

[1] Bassi, F. and Botti, L. and Colombo, A. and Crivellini, A. and Ghidoni, A. and Nigro, A. and Rebay, S., *Time Integration in the Discontinuous Galerkin Code MIGALE - Unsteady Problems*, Notes on Numerical Fluid Mechanics and Multidisciplinary Design 128, 2015.

[2] G. Noventa and F. Massa and F. Bassi and A. Colombo and N. Franchina and A. Ghidoni, *A high-order Discontinuous Galerkin solver for unsteady incompressible turbulent flows*, Computers & Fluids 139, 2016.

[3] F.C. Massa and G. Noventa and M. Lorini and F. Bassi and A. Ghidoni, *High-order linearly implicit two-step peer schemes for the discontinuous Galerkin solution of the incompressible Navier-Stokes equations*, Computers & Fluids 162, 2018.

[4] Carpenter, M. H. and Kennedy, C. A. and Bijl, Hester and Viken, S. A. and Vatsa, Veer N., *Fourth-Order Runge-Kutta Schemes for Fluid Mechanics Applications*, J. Sci. Comput. 25, 2005.

[5] Lang, J. and Teleaga, D., *Towards a Fully Space-Time Adaptive FEM for Magnetoquasistatics*, Magnetics, IEEE Transactions on 44, 2008.

[6] F. Steinebach, *Order reduction of ROW methods for DAEs and method of lines applications*, Techn. Hochsch., Fachbereich Mathematik, 1995.

[7] F. Bassi and A. Ghidoni and A. Perbellini and S. Rebay and A. Crivellini and N. Franchina and M. Savini, *A high-order Discontinuous Galerkin solver for the incompressible RANS and $k-\omega$ turbulence model equations*, Computers & Fluids 98, 2014.

[8] G. Soderlind and L. Wang, *Adaptive time-stepping and computational stability*, Journal of Computational and Applied Mathematics 185, 2006.

[9] Soderlind G., *Digital Filters in Adaptive Time-stepping*, ACM Trans. Math. Softw 29, 2003.

[10] E. Hairer and G. Wanner, *Solving Ordinary Differential Equations II*, Springer Series in Computational Mathematics, 1996.

[11] K. Gustafsson, M. Lundh, G. Sderlind, *A PI Stepsize Control for the Numerical Solution of Ordinary Differential Equations*, BIT 28, 1988.

[12] Simmendinger C. and Versick D., *Integrated Performance Analysis of Computer Systems (IPACS). Benchmarks for Distributed Computer Systems*, Praxis der Informationsverarbeitung und Kommunikation 28, 2005.